2008

Records of natural fires and the Sorption of Polycyclic Aromatic Hydrocarbons (PAHs) by Black Carbon and Carbon Chars in sediments from Oriole Lake (Sequoia National Park)

Kevyn Bollinger
University of Rhode Island, Kevyn.A.Bollinger@gmail.com

Kevyn Bollinger
Ocean Engineering, German Language and Literature
Kevyn.A.Bollinger@gmail.com

Records of natural fires and the Sorption of Polycyclic Aromatic Hydrocarbons (PAHs) by Black Carbon and Carbon Chars in sediments from Oriole Lake (Sequoia National Park)

Faculty Sponsor: Rainer Lohmann, Graduate School of Oceanography, URI

Abstract:

This project investigates the interaction between Black Carbon and Polycyclic Aromatic Hydrocarbons (PAHs) in lake sediments from Oriole Lake in Sequoia National Park California. The interaction between Black Carbon and PAHs is of interest because little is known with respect to the availability and the time scale within which black carbon adsorbs PAHs in a natural system. Black Carbon and PAHs both will eventually be degraded in the environment but the relevant timescales of sorption and degradation are unknown. Field work for this project was conducted July 16-21, 2007 at Oriole Lake in Sequoia National Park California. Sequoia National Park provides a unique environment for PAH and Black Carbon research in that its frequent natural fires are recorded in the giant Sequoias and in Park Service records. The relative isolation of Oriole Lake allowed for a clear sediment record that was primarily influenced by regional scale fire events. A strong correlation in the sediment of Black Carbon percentages to the historical recorded of local fires around Oriole Lake was found. Total PAHs showed neither a trend with time nor with Black Carbon Percentage, suggesting that in this sediment core the PAHs are not strongly bound by the Black Carbon. This project confirmed that Oriole Lake is indeed a prime location for analysis of PAH/ Black Carbon interactions and has provided the starting point for future research on the fire history of the Oriole Lake Watershed.

Keywords: Sediment Record, Black Carbon, Sequoia National Forest

Introduction:

Combustion processes are the source of a vast majority of Polycyclic Aromatic Hydrocarbons (PAHs) to the environment. PAHs are a type of Persistent Organic Pollutant (POP) and have various harmful effects in nature and to Humans. Oil derived PAHs (petrogenic) are also abundant in nature from natural sources and from man-

made pollution of spilled petrol fuel. The combustion derived PAHs (pyrogenic) are formed from natural sources such as forest fires as well as from human based activities that burn carbonaceous fuels (e.g., wood, oil, coal and diesel gasoline). The same combustion processes that produce these PAHs also release Black Carbon. Black Carbon is a byproduct of incomplete combustion (such as in the black plume from diesel engines in buses and trucks). Incidentally, black carbon (also known as soot, char, charcoal, etc.) adsorbs organic compounds including PAHs. Therefore, the same combustions processes that release harmful PAHs also produce a substance that may reduce their availability in the environment.

Previous studies have demonstrated that black carbon adsorbs PAHs in the laboratory and in impacted harbor sediments. Little is known with respect to the availability and the time scale within which black carbon adsorbs PAHs from the natural system. Black Carbon and PAHs both will eventually be degraded in the environment but the relevant timescales of sorption and degradation are unknown.

PAHs are not only produced through combustion processes, as there are petrogenic and natural sources. However, through the use of various ratios between certain key PAH compounds the source(s) of the PAHs in a sample can be determined.

Field work for this project was conducted July 16-21, 2007 at Oriole Lake in Sequoia National Park California. Three Livingston sediment cores were taken in approximate 1m sections up to 5 meters in depth when bedrock/ glacial till were struck. Five sediment biological cores of the first 1+m with intact sediment-water interfaces were also taken. This paper presents the analysis of the third taken of the Biological cores, OL07-BC3 (Oriole Lake 2007-Biological Core Three).

Sequoia National Park provides a unique environment for PAH and Black Carbon research in that its frequent natural fires are recorded in the giant Sequoias. From the tree record the fire record for the past 400 years is known. Smaller scale fires not resulting in scaring on trees have also been recorded by the park service since 1900. Having this fire recorded provides a unique opportunity to reference the sediment layers to a known fire chronology. Additionally Oriole Lake is remote and provides a location minimally influenced by events outside the immediate geographic region of the lake. The relative isolation of Oriole Lake should allow for a clear sediment record that can be easily compared to the burn history of the region, thus enabling the analysis of PAH and Black Carbon interactions over time. The goals of this project were (i) to correlate the sediment to the burn record; (ii) to determine if there is evidence of PAH and Black Carbon interactions; (iii) and on what time scale the sorptive capacity of the BC to retain PAHs is lost. This work will help in better understanding how pollutants cycle through the environment and how long they persist.

Sampling and Laboratory Procedures:

Biological Sediment Core: Biological sediment cores are taken by a sampling tube with a piston inside which has an attached line extending through the top of the sampling tube. The depth of the lake at the point of sampling was determined with a plumb line. The sampling tube was then extended towards the lake bottom on a rod. The line to the piston was tied off so that the piston inside the sampling tube would remain at the predetermined depth just above the lake bottom. The sampling tube is then pushed down into the soft sediment bottom. The piston creates a seal above the sediment water interface which helps prevent the sediment core from sliding out of the sampling tube as the device is pulled up to the surface. The core captures the sediment water interface but has the disadvantage of only being able to sample the top soft layer of the sediment.

The cores taken in California were capped and shipped to Rhode Island vertically in a shipping crate to preserve the sediment water interface as much as possible. It was unknown to what extent the interface was disturbed during the shipping process. At the University of Rhode Island the core was placed in a stand and extruded vertically from the sampling tube. Each centimeter was spooned/ sliced off depending on the consistency and stored in individual sampling jars. All equipment used was rinsed with distilled water and wiped clean with KimWipes® between each sample. The field log book and lab book pages relevant to these processes can be found in Appendix A.

Sample preparation (35˚C Drying): Each sample was homogenized and approximately half of the sample was weighed out onto a foil pan and placed in a drying oven at 35˚C for approximately 48 hours. The dry weight was then taken and used to determine the percent water content of the original sample. The dried samples were ground with a mortar and pestle and then sieved with a #40 US Standard sieve (425µm). They were then split into three parts: about 1-1.4 g per sample were packaged and sent to Liverpool University for ^{210}Pb dating. Approximately ~0.15 g was used for the 725 ˚C oxidation (loss on ignition), and ~0.08g for the 375˚C oxidation to determine soot black carbon. The remaining wet half of the original sample was used for PAH analysis.

Radiometric Dating: Dry sieved samples were sent to Peter Appleby (Liverpool University, United Kingdom) for radiometric dating based on ^{210}Pb and ^{137}Cs.

Black Carbon (375˚C oxidation): The total organic carbon (TOC) percentage consists of partially of organic carbon (OC) and partially of black carbon (BC). Samples were spread thinly in prebaked 2ml vials and oxidized at 375˚C under air flow (Compressed Air, Airgas Inc.) in a Barnstead Thermolyne 47900 Furnace. The sample vials were weighed before samples were added, before oxidization, and after oxidization. BC was isolated in this process from OC due to a difference in oxidization temperature. From the difference in mass before and after the oxidization process the percentage of OC

was found. BC constituted the remaining carbon in the sample. The BC percent and isotope ration was determined by a Carlo Erba NA 1500 series II Elemental Analyzer attached to a continuous flow isotope ratio Micromass Optima spectrometer at the EPA operated by Mark Cantwell.

Loss on ignition (725˚C oxidation): The samples were spread thinly in pre-baked crucibles and then oxidized at 725˚C for 24 hrs in a Barnstead Thermolyne 47900 Furnace. The difference in mass before and after the oxidization process yielded the percent of total combustible mass in the sample.

Polycyclic Aromatic Hydrocarbons (PAH) Analysis: The wet sediment sample was weighed out into a pre-rinsed Teflon test tube with a screw on cap. Internal standard and 15 ml acetonitrile were added to the sediment and the test tube was capped and hand agitated. 10 ml of hexane was then added and the capped test tube was placed in a metabolic shaker at 65˚C for one hour. 10 ml clean water was then added. The following was then repeated three times: the test tube was shaken, centrifuged, the top layer (hexane) was pipetted off into a round bottom flask, and 10 ml hexane was added. The combined extracts were then rotorary-evaporated down to a about 5ml. Activated copper was added to the sample and let stand for at least one hour or overnight to remove sulfur in the sample. Sodium Sulfate was added to remove any residual water in the sample and the liquid was then pipetted off and sent through hexane-cleaned Sep-Paks® which contain silicic acid. The collected liquid was rotorary-evaporated down to 20-30µL and transferred to GC vials where the injection standard was then added.

Samples were analyzed for PAHs on an Agilent 6800 chromatograph (GC) in series with an Agilent 5973N mass spectrometer (MS) operated in the negative electronic ionization mode. For each sample, 1 µL was injected in the splitless mode onto a Varian Factor Four VF-5MS column (30 m, internal diameter 250 µm). Column flow was constant at 2 mL/min. The temperature (T) program was as follows: hold 60 °C for 3 min, increase to 120 °C at 3.5 °C/min, increase to 315 °C at 8 °C/min, and hold for 8 min. The injection port was maintained at 300 °C, and the MS transfer line at 280 °C.

Native PAH concentrations in the sample were found in relation to the nearest eluting deuterated calibration standard. Native PAHs in known but varying concentrations in five injection standards were used to establish the calibration curve for GC-MS response to actual concentrations. The concentration of natives in a sample was calculated as a ratio of the response of the known concentration of the deuterated PAH internal standard compounds. The concentration was adjusted to account for the calibration factor found from the injection standard. An example of these calculations performed in excel spreadsheets can be found in Appendix B.

Summary of Lab Procedures: The following flow chart (Figure 1) shows the analysis that was performed on each sample from the sediment core. The central column of the flow chart details a process to determine char percentages that was not conducted during this project but which will be performed at a later date in further research on the Oriole Lake cores.

Figure 1. Flow Diagram of Lab procedures.

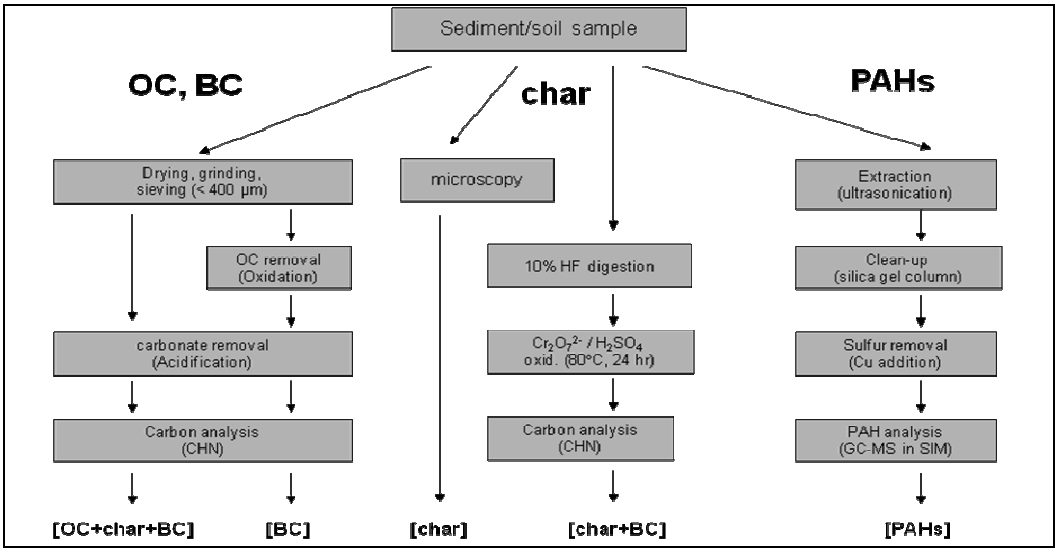

Data and Results:

Radiometric Dating: The results of the ^{210}Pb and ^{137}Cs dating as of May, 2008 were inconclusive. Peter Applebee reported that the ^{210}Pb were reduced by half at 32 cm, suggesting that the top 32 cm only covered 2 or 3 decades which seemed highly unlikely. The ^{137}Cs was also puzzling to Peter Applebee in that the highest values occurred in the top 10 cm but then steadily decreased with depth. The results seemed inconclusive and Peter Applebee is planning on testing the samples down farther to 42cm. He hypothesized that the low dry bulk density (high water content) may have distorted the ^{137}Cs record by post-depositional migration.

Another indication of the age of these sediments came from previous work on a core taken from Oriole Lake in 1987 by Margaret Davis (University of Minnesota). Her research indicated that the top 37 cm were 90 years old, suggesting that the top 43cm analyzed by in this project would be around 105 years old. This time scale serves as a rough guidance only, due to differences in sedimentation rates between Margaret Davis' core site and this projects core site.

Fire Record: There were two ways in which a composite fire record of the local region around Oriole Lake was found: tree ring scaring and park service documentation. Tree ring scaring relies on scars found in tree rings to determine when fires occurred. This method requires multiple tree bores or cross-sections to determine the entire record as each tree may not have been scared from every single fire. This method is limited to regions were the trees are fire resistant enough to survive a fire. The tree ring scaring gives no indication of fires that were too small to cause scaring or that were too big and burned the entire tree. This method does however provide a fire history that goes back many centuries before documentation of fires began. A picture showing scaring on a tree cross-section can be found in Appendix D. A composite time line from several different trees in the Oriole Lake grove has been compiled by Tony Caprio of the US NPS, Sequoia and Kings Canyon National Park. The timeline of events recorded in tree rings is shown in Figure 2.

Figure 2. Oriole Lake Grove tree ring record of fire events (Caprio 2008)

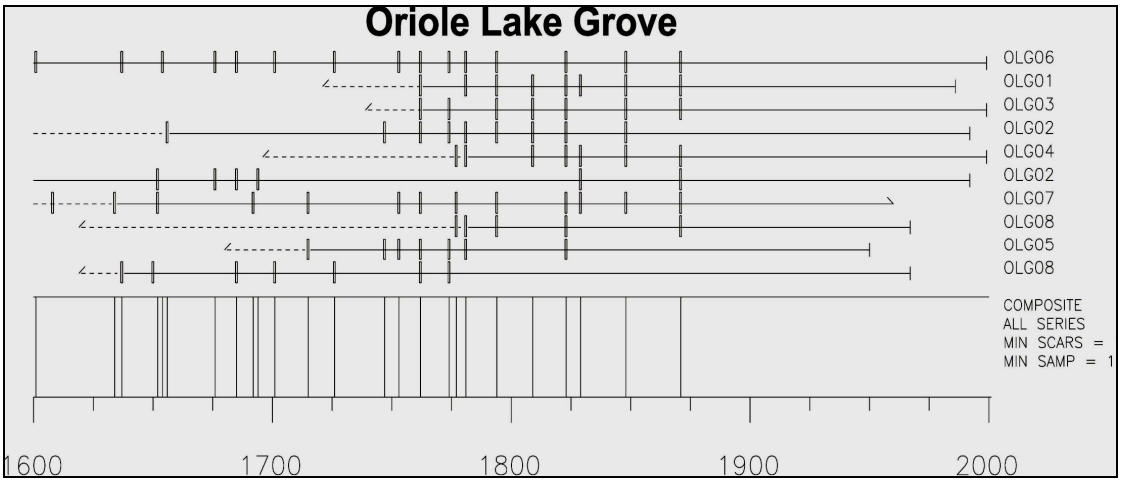

The fire record developed from tree rings indicates that there have been no fires near Oriole Lake since 1870. This record does not include fires that were not located directly in the vicinity of Oriole Lake or at a lower elevation where scrub forests dominate and no trees would survive a burn. Since the dating records indicated that the top 43cm analysis in this project is around 100 years, the fires shown in the tree ring record would not appear in the sediment section analysed.

The local recorded history of the region around Oriole Lake was retrieved from forest service records and publications. This recorded history is limited to recent events of the last century. These records provide detailed information of where the burns were located, what year they occurred in, and what the size of the burn area was. The records however give no indication to the influence of these events on the Black Carbon flux into Oriole Lake. This would depend on the distance of the burn from the lake, the prevailing winds at the time of the burn, the size of the burn, and the

topography of the region between the burn site and Oriole Lake. A map of the burn record for the Mineral King watershed (Caprio et al., 1997) has been overlaid onto a contour map of the region. Figure 3 shows the locations of these recorded burns and the location of Oriole Lake. The original map of the historic burns in the Mineral king watershed can be found in Appendix D.

Figure 3. Mineral Kings Watershed burn record overlaid on a topographic map. Oriole Lake is shown with a green arrow. (Caprio et al. 1997)

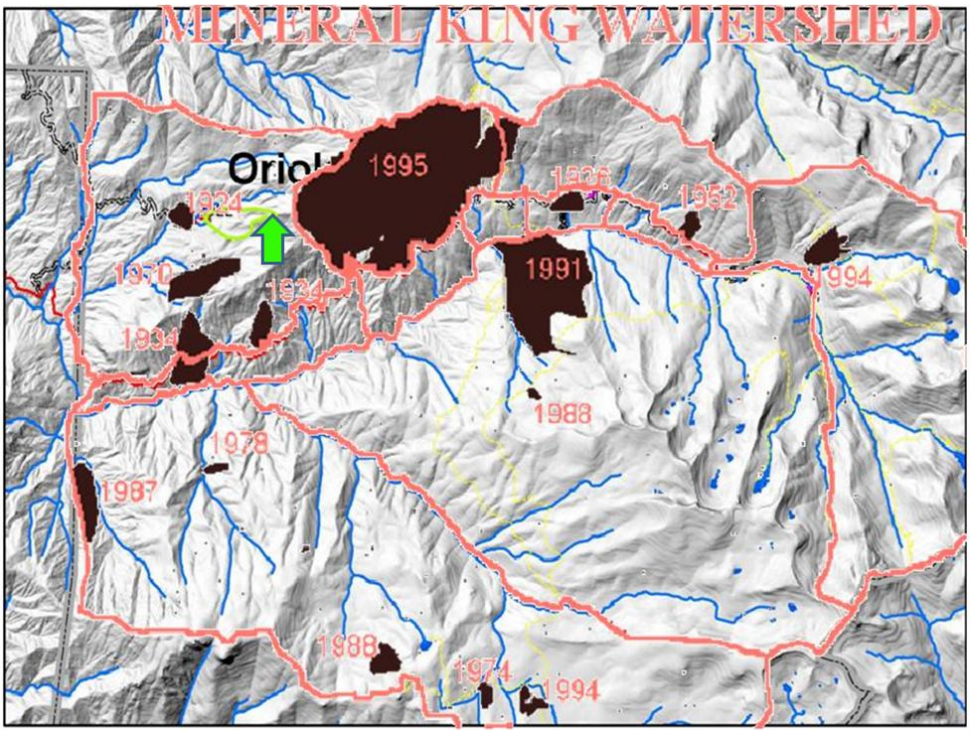

Westerly winds are prevailing at Oriole Lake . The influence each of the burn areas in Figure 3 on Oriole Lake can be estimated based on westerly winds, the burn size and the topography. Values of 1 to 10 were assigned to each burn based on the estimated magnitude of influence each burn should have. The burn in 1991 for example was assigned a value of 5 since it is downwind and on the other side of a ridgeline but is quite a large burn. The burn in 1934 is significantly smaller and also on the opposite side of a ridgeline from Oriole Lake but received the same value since it was located slightly upwind. All of the burns immediately in the vicinity of Oriole Lake received influence factors of 10 on Oriole Lake. This record of the Mineral king watershed is not the complete influence of local fires on Oriole Lake. Another paper by the forest service resulted in Figure 4 which shows burned areas on a two decade time scale.

Figure 4. Lower Sequoia and Kings Canyon National Park burn record on a two decade time scale. The box in red indicates the Mineral King watershed and the green arrow Oriole Lake. (USDA Forest Service, 2004)

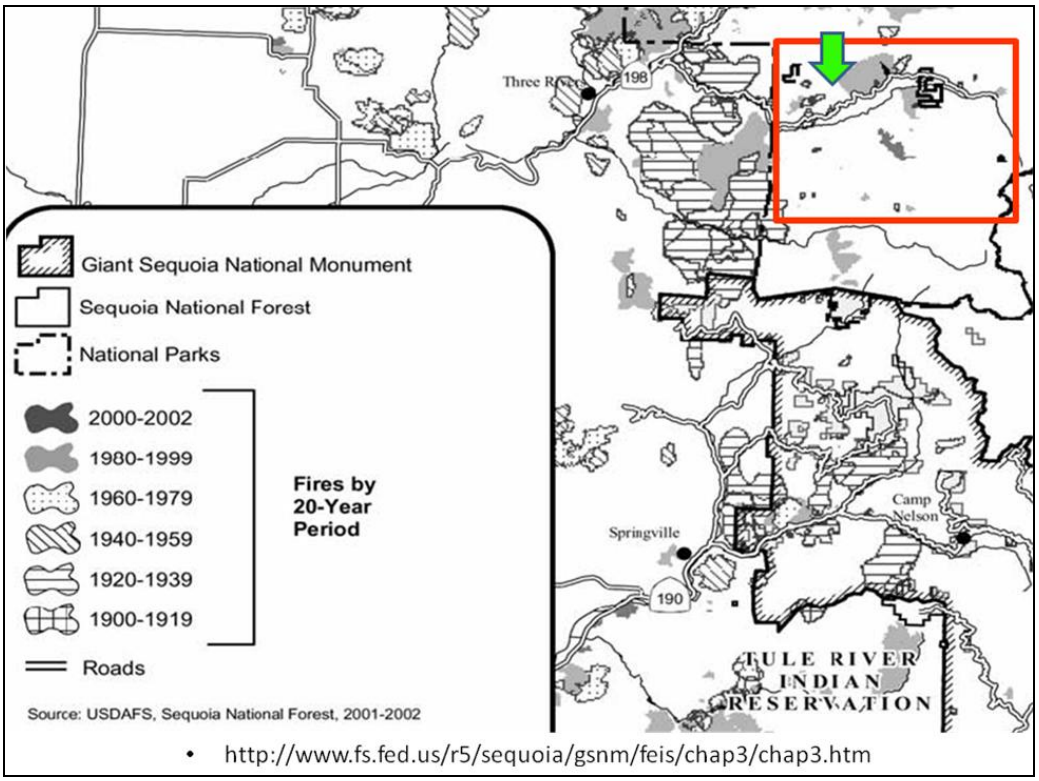

From Figure 4 it can be seen that there were very small fires next to Oriole Lake from 2000-2002. Figure 3 was published in 1997 so those fires need to be accounted for in addition to the fires already considered within the watershed and would have a very large influence on the Lake. Outside of the Mineral King Watershed it can be seen that large areas burned upwind of Oriole Lake during the 1920-30s, the 1940-50s, and the 1980-90s. To determine the possible influence of these burn areas, the topography between the burn areas and Oriole Lake needs to be considered. Figure 5 is a topographic googlemap® image looking due west (upwind) and showing the location of Oriole Lake with respect to the burn locations.

Figure 5. Topographic googlemap® image looking due west (upwind) and showing the location of Oriole Lake with respect to the burn locations.

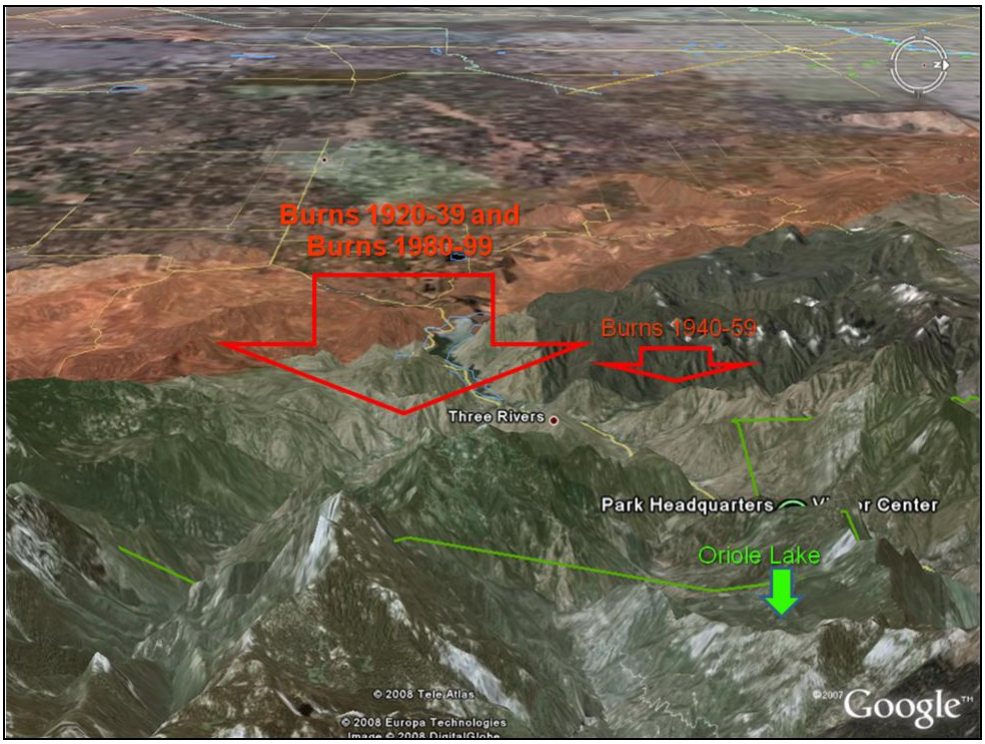

From this map it can be seen that the burns in the 1920-30s and the 1980-90s occurred predominantly behind a large ridgeline from Oriole Lake or on the ridge line at a higher elevation than the lake. This would suggest that aerosols from those fires would have been channeled away from Oriole Lake or would have been higher in elevation and carried away by the prevailing winds. The burns in the 1980-90s did also have some burn areas in the valley due west of Oriole Lake near the Park Entrances but as can be seen in Figure 5 there is a smaller ridgeline north and northwest of oriole lake between those burns and the lake. Therefore, all of the burns recorded in the 1920-30s and 1980-90s would have minimal impact on the lake. The burns in the 1940-50s however can be seen to be in the valley directly upwind of Oriole Lake at a similar or slightly lower elevation and with no large geographic feature blocking the wind. These burns, though significant, occurred far away and would not have the same impact as burns in the immediate vicinity of the lake. For the influence of the burns in the two decade spans, the entire baseline of influence was increased since specific years of the fires within the two decade span are not known. A table of the given influence factor per year from 1900 to 2007 can be found in Appendix D. The following figure shows a plot of the estimated influence by year of historic burns on the Black Carbon flux into Oriole Lake.

Figure 6. Estimated fire record influence by year on Oriole Lake.

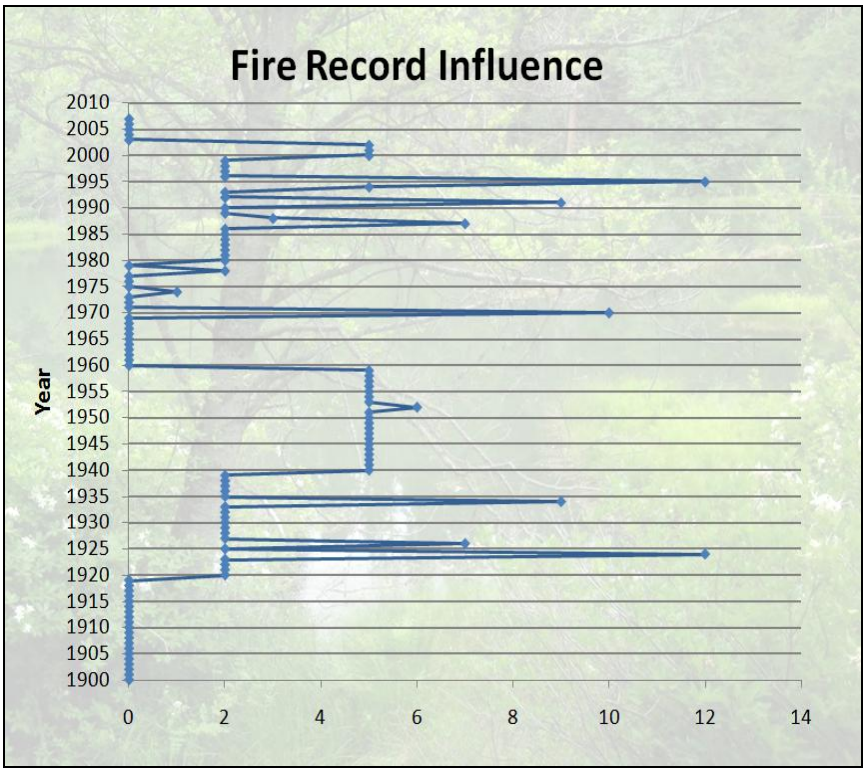

It should be noted that within the decades with raised base lines, the fires that those raised baselines represent would actually occur as spikes somewhere within the two decade span of that increased baseline. It does not indicate that the regions in questions burned continually for the two decade span and the raised baseline is only a means of visualizing these influences with unknown dates of occurrence. The estimated Black Carbon Flux into Oriole Lake form local fires can then be compared with the measured Black Carbon percentages in the sediment with depth.

Carbon Analysis: The results of the various drying and oxidizing procedures to determine the water content (%w), the Total Organic Matter (TOM), the percent Organic Carbon (OC), the percent Black Carbon (BC), and the Loss on Ignition (LOI) are shown in Appendix E. The results adhere to general rule-of-thumb ratios. The OC (~20%) was approximately half of the TOM (~40%) since carbon makes up about half of the molecular weight of organic compounds. The difference in TOM (~40%) and LOI (~42%) is the percent of organic compounds in the Black Carbon form (~2%). The percent Black Carbon is approximately half of that (~1%) for the same reason OC is about half the TOM. In the thermal oxidization process to isolate Black Carbon, insufficient oxygen can cause the conversion of OC to BC. This would result in a bias towards BC, and would manifest itself in a positive correlation between OC and apparent BC. This bias was not observed for our samples (Appendix E) which indicates that the oxidization method fully combusted OC. Various standard reference materials were run with the samples and the Black Carbon percentages for the reference materials were close to those found in previous studies (Appendix C). The percent Black Carbon with depth is shown in Figure 7.

Figure 7. Percent Black Carbon with depth.

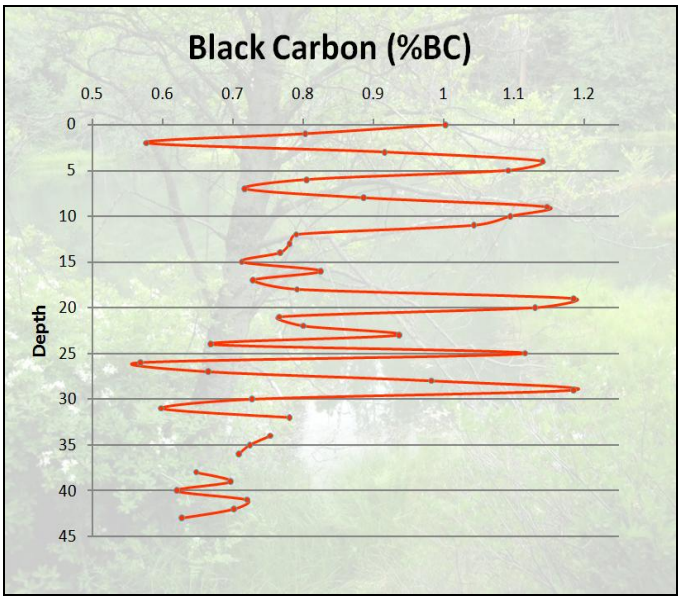

The measured Black Carbon in the sediment can then be compared with the estimated influence of regional fires on the Black Carbon flux into Oriole Lake as shown in Figure 8.

Figure 8. The fire record influence on Oriole Lake compared to measured Black Carbon values.

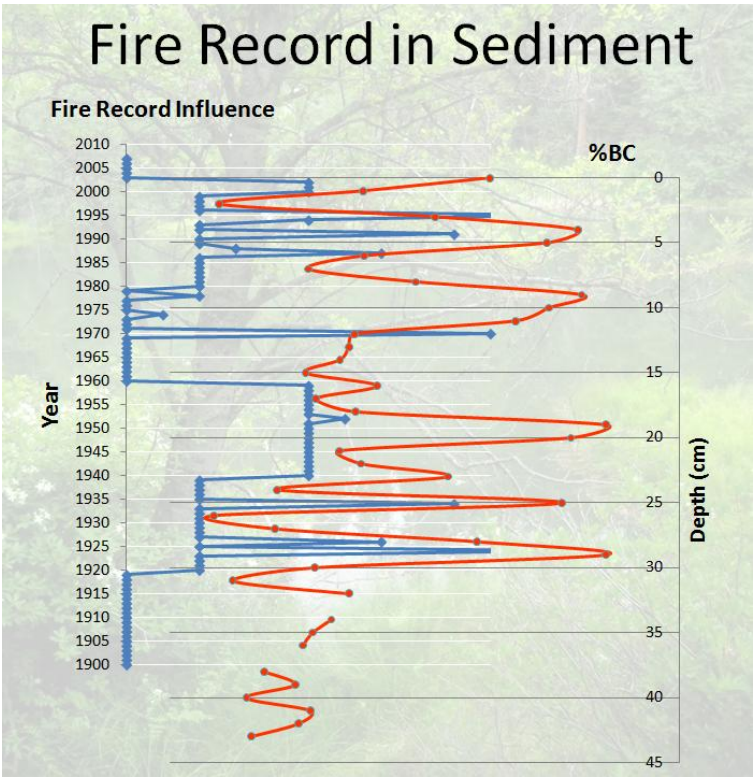

There is a strong correlation between the estimation based on fire records and the measured Black Carbon (Figure 8), although the influence of historical local burns is based on numerous assumptions such as wind direction and effective aerosol transport distance. Figure 8 suggests that the top 1 to 1.5 cm of the sediment column was lost in the coring process and that the 43 cm analyzed covered a time scale of approximately 120 years. This compares well to the previous estimation of around 105 year, which can be explained by a higher compactation of the sediment at larger depths and/or differences in coring locations in Oriole Lake.

PAH Extraction Results: A sample data chart of the PAH analysis process can be found in Appendix B. Graphs of ratios of significant PAHs and the total PAHs concentration in the sediment (in nanograms per gram of dry sediment) can be seen in Figure 9.

Figure 9. Selected PAH ratios and results.

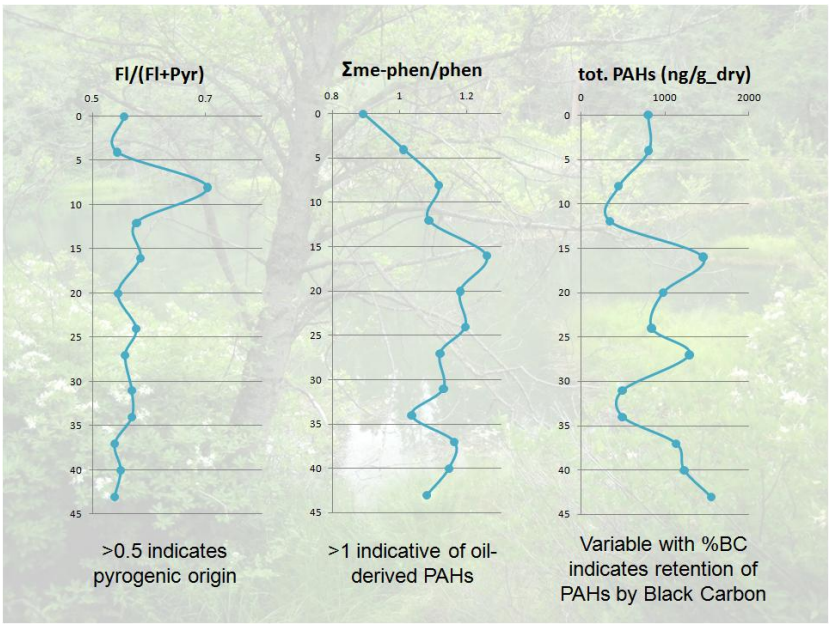

The ratio of Flouranthene over Flouranthene plus Pyrene greater than 0.5 indicates a pyrogenic (burning) origin. Figure 9 shows that at all depths the PAH source is from burning processes. A ratio of Methylated Phenanthrenes over Phenanthrene greater than 1 is indicative of oil derived PAHs. The ratio in the sediment is not significantly greater than one to definitively indicate oil derivation. It is conceivable that Phenanthrene degrades faster in nature than Methylphenanthrenes which would artificially increase the ratio. If the ratio is entirely accurate, Figure 9 could indicate an increase in oil derived PAHs until 1960 (16cm depth) and then a decrease in oil derivation afterwards. This could be placed in historical context with the passing of the Clean Air acts in the 1960s. Taken together, the PAH results indicate that the Black Carbon flux in Oriole Lake is heavily dominated by natural fires and is minimally

impacted by sources outside of the regional scale. The total PAHs compared to the percent Black Carbon is shown in Figure 10.

Figure 10. Total PAH comparison to Black Carbon percent.

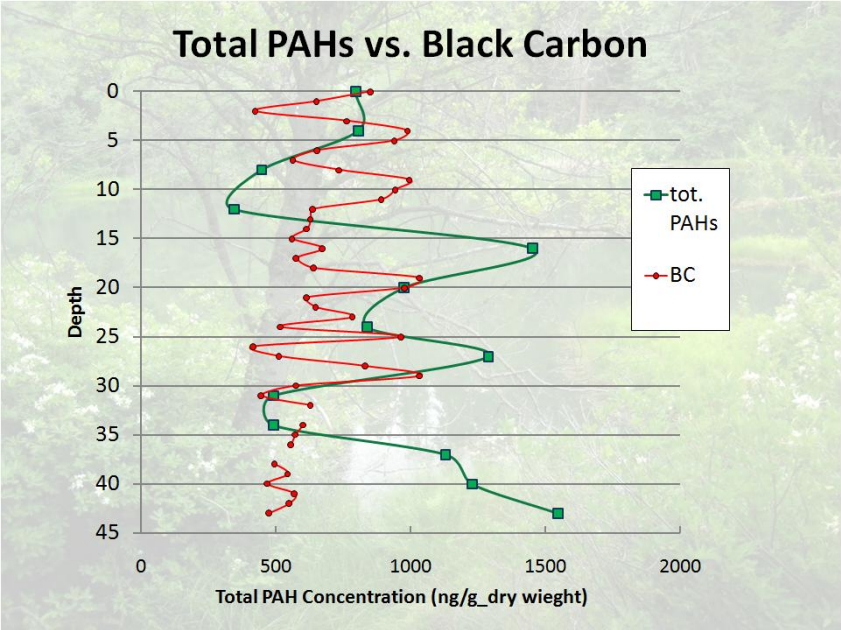

Total PAHs show no trend with time and no trend with Black Carbon Percentage, suggesting that in this sediment core the PAHs are not strongly bound by the Black Carbon. The upper 43cm of the sediment column that was analyzed did however have a very high water content which could have caused migration of compounds in the sediment column.

Conclusions:

There is a strong correlation in the sediment record of Black Carbon percentages to the historical recorded of local fires around Oriole Lake. Fire histories have been compiled from historical records and tree ring scaring to give an accurate fire history record back to 1600. Oriole Lake is indeed remote enough that the Black Carbon fluxes are primarily determined by local influences on the lake. No evidences of retention of PAHs by Black Carbon was observed in the top 43cm of the sediment column but the high water content may affect the interaction of PAHs and Black Carbon. This project confirmed that Oriole Lake is indeed a prime location for analysis of PAH/ Black Carbon interactions and has provided the starting point for future research on the Oriole Lake cores which could be undertaken for a Master's thesis by a GSO student.

Future Work:

The project to date has analyzed the top 43cm of one of the five biological cores. In addition, there are three Livingston cores which are each approximately 4.5m deep.

Further work should extend the results to earlier in history. The PAH ratios and correlation between total PAHs and Black Carbon may be more conclusive at greater depths. Future work should determine how PAHs are sorbed by black carbon. If there is a correlation, the last 200 years record in the sediment during industrialization can be more closely looked at. By removing contributions of black carbon and PAHs due to natural processes, the impact of manmade processes could be examined.

Acknowledgments:

I would like to thank my Faculty Advisor, Rainer Lohmann, for his extensive help and support on this project and for the opportunity to conduct field research in Sequoia National Forest, California. I would also like to thank Mark Cantwell at the EPA for his invaluable and well timed aid in running many samples in the EPA's CHN Anlyzer. I would like to thank John King and his lab group (especially Clifford Heil and Nathan Vinhateiro) at the Graduate School of Oceanography, URI for their help with field work in Sequoia National Forest and with core handling at GSO. Lastly, I would like to recognize the contributions of Tony Caprio and the rest of the Park Service Staff who helped us at Sequoia and Kings Canyon National Park.

References:

Caprio, Anthony C., Clarence M. Conover, MaryBeth Keifer, and Pat Lineback. Fire Management and GIS: A Framework for Identifying and Prioritizing Fire Planning Needs. 1997. <http://www.nps.gov/archive/seki/fire/frid97.htm>

Caprio, Anthony C. Personal Communication. US NPS, SEKI. 2008

Lohmann, Rainer, Kevyn Bollinger, Mark Cantwell, Irene Fischer-Bruns, Johann Feichter, Matthias Zabel. Fluxes of soot black carbon to South Atlantic Sediments. Submitted to Global Dispersal Cycles, May 2008.

USDA Forest Service. Giant Sequoia National Monument Management Plan. July 2004. <http://www.fs.fed.us/r5/sequoia/gsnm/feis/chap3/chap3.htm>

Appendix A: Field log book information for biological sediment core OL07-BC3.

WED. 7/18/07

ORIOLE LAKE, SEQ. NAT. PARK

SURFACE CORES

CORE: OLØ7-BC1
WATER DEPTH - 23 ft.
CORE LENGTH: [redacted] 139 cm

CORE: OLØ7-BC2
CORE LENGTH: 127 cm

CORE: OLØ7-BC3
CORE LENGTH: 124 cm

CORE: OLØ7-BC4
10' ABS LINER

CORE: OLØ7-BC5
10' ABS LINER
CORE LENGTH: ~200 cm

THURS. 7/19/07

ORIOLE LAKE (CONT.)

LIVINGSTONE CORES

SITE 1
WATER DEPTH: 718 [redacted] cm
TOP OF CASING: 55 cm from water surface
TOTAL CASING LENGTH: 915 cm

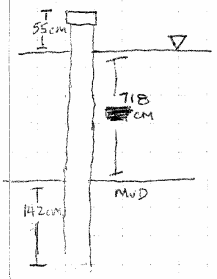

LENGTH OF CORER: 149 cm
LENGTH OF PUSH ROD: 305 cm 1
" 2
" 3

Appendix B: Sample data chart for PAH analysis

Sample sheet

Sample Name	43-44	%w=	1458.111	W-tt=	33.9339	W -w/Sed=	65.4695									
Data File																
COMPOUND	**m/z**	**Ret Time**	**Area**	**Aint/Anat**	**slope**	**Intercept**	**ng in samp**	**ng/g_dry**	**Diff from Std**	**Diff from Std in "C"**	**Diff of Diffs**					
Naphthalene	128	14.450	39455	56.66770	0.20133	0.451226398	1.798	0.888	10.403	10.365	0.038					
2-Methylnaphthalene	142	18.282	15231	146.79430	0.36525	0.693514414	1.259	0.622	6.571	6.578	0.007					
1-Methylnaphthalene	142	18.861	11078	201.82560	2.30044	14.20193832	5.767	2.850	5.992	5.992	0.000		Deploy Date			
Biphenyl	154	21.386	28118	79.51576	0.39479	0.737760676	2.512	1.241	3.467	3.487	0.020					
Acenaphthylene	152	23.942	4050	552.05531	0.38341	0.170322109	0.351	0.174	0.911	0.937	0.026		Vol		conc	
Acenaphthene-d10	*164*	**24.853**	**2235824**	**8.61220**	**1.67189**	**-0.133876872**	253.747		**-11.227**	-11.220	**0.007**	**Internal**	**100**		**5.06**	**ng/ul**
Acenaphthene	154	25.010	3763	594.15998	29.9624	52.07725916	25.517	12.607	-0.157	-0.150	0.007					
Flourene	166	27.384	53718	65.77402	0.59931	0.889131992	4.610	2.278	3.397	3.410	0.013	native		ul		ng/ul
Phenanthrene-d10	*188*	**30.781**	**3533249**	**5.44976**	**0.92578**	**-0.025335342**	222.044		**-5.299**	-5.299	**0.000**					
Phenanthrene	178	30.846	156716	22.54555	0.80386	1.14724598	18.041	8.914	-0.065	-0.078	0.013	Injection	30	ul	43.57	ng/ul
Anthracene	178	31.008	12366	285.72287	0.46192	0.379877774	0.818	0.404	-0.227	-0.227	0.000					
3-Methylphenanthrene	192	32.537	39016	90.55898	0.462	0.38	2.581	1.275	-1.756	30.781	32.537	Recovery				
2-Methylphenanthrene	192	32.609	24096	146.63218	0.462	0.38	1.594	0.788	-1.828	30.781	32.609	Acenaphthene-d10		50.147677		
9-Methylphenanthrene	192	32.902	78867	44.80009	0.462	0.38	5.218	2.578	-2.121	-1.880	0.241	Phenanthrene-d10		43.882251		
1-Methylphenanthrene	192	32.934	152768	23.12820	0.462	0.38	10.108	4.994	-2.153	-1.971	0.182	Chrysene-d12		44.131404		
Flouranthene	202	34.660	155104	22.77987	0.4611	0.609861768	10.242	5.061	1.420	1.414	0.006	Perylene-d12		38.047112		
Pyrene	202	35.302	112872	31.30315	0.24452	0.916375922	3.952	1.953	0.778	0.783	0.005					
p-Terphenyl-d14	*244*	**36.080**	**19255371**	**1.00000**	**0**	**0**	480.308		**0.000**	0.000	**0.000**					
Retene	234	36.488	12045297	0.28771	1.53704	2.998173054	2703.228	1335.611	-0.408	-0.392	0.016					
Benz[a]anthracene	228	38.963	78817	43.96954	4.29547	2.040033277	49.432	24.423	0.038	0.032	0.006					
Chrysene-d12	*240*	**39.001**	**3465547**	**5.55623**	**0.94923**	**0.047834062**	223.305		**-6.447**	2.915	**9.362**					
Chrysene	228	39.126	68352	50.70147	0.47002	0.663379329	4.691	2.318	-0.125	-0.071	0.054					
Benzo[b]flouranthene	252	41.991	177607	19.51245	0.83878	0.201661186	21.751	10.747	0.909	0.944	0.035					
Benzo[k]flouranthene	252			#DIV/0!	0.39162	0.519965519	#DIV/0!		42.900	0.879	42.021					
Benzo[e]pyrene	252	42.634	71996	48.13527	0.95181	0.447828057	10.005	4.944	0.266	42.892	42.626					
Benzo[a]pyrene	252	42.752	40998	84.52966	0.95181	0.447828057	5.698	2.815	0.148	0.149	0.001					
Perylene-d12	*264*	**42.900**	**2289386**	**8.41071**	**1.23879**	**0.089064106**	192.518		**6.820**	6.812	**0.008**					
Perylene	252	42.957	3314644	0.69069	0.30088	0.425777654	220.424	108.907	-0.057	-0.061	0.004					
Indeno[1,2,3-cd]pyrene	276	45.370	90292	25.35536	0.66344	0.171599598	13.240	6.541	-2.470	-2.460	0.010					
Dibenz[a,h]anthracene	278	45.448	4384	522.21396	1.22991	-0.160506629	1.192	0.589	-2.548	-2.539	0.009					
Benzo[ghi]perylene	276	45.886	138059	16.58266	0.32269	0.296974851	9.847	4.865	-2.986	-2.911	0.075					
				tot. PAHs	e-phen/pt	FI/(FI+Pyr)	Retene	%Retene								
				1548.387	1.081	0.538	1335.611	0.863								

Standards Sheet

	0.071	0.454	1.993	5.268	13.880	30.951										
[Inj]/[Int]	13.651	2.138	0.487	0.184	0.070	0.031				**Percent Increase**						
										14.248	24.668	37.778	58.957	45.849	Median	
COMPOUND	**B**	**C**	**D**	**E**	**F**	**G**	**slope**	**intercept**	**r2**	**B to C**	**C to D**	**D to E**	**E to F**	**F to G**		
Naphthalene	0.028	0.199	0.601	2.161	4.103	6.210	0.201	0.451	0.943	14.015	33.052	27.801	52.664	66.069		
2-Methylnaphthalene	0.039	0.312	0.936	3.660	7.227	11.205	0.365	0.694	0.952	12.435	33.347	25.574	50.642	64.498		
1-Methylnaphthalene	1.634	7.912	18.789	48.114	49.473	80.332	2.300	14.202	0.840	20.651	42.108	39.052	97.252	61.585		
Biphenyl	0.044	0.355	0.990	3.865	7.860	12.087	0.395	0.738	0.952	12.266	35.838	25.616	49.17	65.029		
Acenaphthylene	0.037	0.253	1.065	2.804	4.801	12.236	0.383	0.170	0.991	14.537	23.736	37.971	58.405	39.241		
Acenaphthene-d10	**22.767**	**2.923**	**0.700**	**0.266**	**0.160**	**0.070**	**1.672**	**-0.134**	**0.999**	**12.84**	**23.934**	**38.082**	**59.957**	**43.966**		
Acenaphthene	5.970	33.149	139.312	301.934	428.192	980.427	29.962	52.077	0.979	18.011	23.795	46.14	70.514	43.674		
Flourene	0.087	0.540	2.181	5.555	9.411	19.095	0.599	0.889	0.986	16.048	24.754	39.259	59.025	49.287		
Phenanthrene-d10	**12.636**	**1.800**	**0.427**	**0.168**	**0.102**	**0.047**	**0.926**	**-0.025**	**1.000**	**14.248**	**23.733**	**39.355**	**60.765**	**45.838**		
Phenanthrene	0.060	0.690	2.880	7.953	11.753	25.843	0.804	1.147	0.981	8.6315	23.964	36.217	67.667	45.478		
Anthracene	0.058	0.370	1.387	3.719	6.315	14.735	0.462	0.380	0.992	15.777	26.712	37.285	58.889	42.858		
3-Methylphenanthrene							0.462	0.380								
2-Methylphenanthrene							0.462	0.380								
9-Methylphenanthrene							0.462	0.380								
1-Methylphenanthrene							0.462	0.380								
Flouranthene	0.042	0.379	1.074	4.364	7.660	14.401	0.461	0.610	0.980	10.976	35.297	24.62	56.966	53.193		
Pyrene	0.050	0.339	1.426	3.625	4.962	7.961	0.245	0.916	0.916	14.725	23.789	39.346	73.071	62.322		
p-Terphenyl-d14	**0.079**	**0.555**	**2.340**	**5.947**	**9.787**	**21.351**				**14.248**	**23.733**	**39.355**	**60.765**	**45.838**		
Retene	0.183	1.448	4.027	17.440	27.542	48.223	1.537	2.998	0.958	12.639	35.964	23.093	63.322	57.113		
Benz[a]anthracene	0.055	0.406	14.501	34.790	50.361	138.141	4.295	2.040	0.980	13.667	2.7966	41.683	69.082	36.456		
Chrysene-d12	**13.001**	**2.105**	**0.528**	**0.199**	**0.120**	**0.055**	**0.949**	**0.048**	**1.000**	**16.19**	**25.068**	**37.745**	**60.215**	**46.036**		
Chrysene	0.075	0.450	1.771	4.372	6.931	15.113	0.470	0.663	0.986	16.742	25.387	40.499	63.084	45.86		
Benzo[b]flouranthene	0.056	0.434	2.001	5.900	10.338	26.615	0.839	0.202	0.992	12.827	21.701	33.922	57.069	38.843		
Benzo[k]flouranthene	0.057	0.343	1.375	3.568	5.868	12.514	0.392	0.520	0.988	16.738	24.916	38.549	60.802	46.891		
Benzo[e]pyrene							0.952	0.448								
Benzo[a]pyrene	0.067	0.531	2.555	7.113	12.253	30.249	0.952	0.448	0.992	12.676	20.766	35.921	58.052	40.506		
Perylene-d12	**16.980**	**2.863**	**0.704**	**0.271**	**0.156**	**0.076**	**1.239**	**0.089**	**1.000**	**16.862**	**24.582**	**38.534**	**57.613**	**48.553**		
Perylene	0.035	0.270	0.733	2.675	5.368	9.306	0.301	0.426	0.977	12.968	36.77	27.405	49.827	57.683		
Indeno[1,2,3-cd]pyrene	0.060	0.331	1.597	4.440	8.581	20.928	0.663	0.172	0.996	18.114	20.737	35.968	51.747	41.001		
Dibenz[a,h]anthracene	0.066	0.536	2.538	7.311	14.499	38.801	1.230	-0.161	0.993	12.303	21.122	34.712	50.426	37.368		
Benzo[ghi]perylene	0.042	0.260	0.994	2.629	4.565	10.272	0.323	0.297	0.993	16.091	26.132	37.81	57.59	44.441		
										14.248	**24.668**	**37.778**	**58.957**	**45.849**	**Median**	
blue - low r2 but acceptable due to considering percent increases																
red- accual slope/intercept for compound not used																

Appendix C: Final compiled data chart with W%, BC, TOC, and PAHs

Oriole Lake- Biological Core 3

OL07-BC3

Water depth 23 feet

initial core length 124 cm

core length just prior to splitting 118.2 cm

OL07-BC3/ x-x cm

| | Extrusion process | | Drying Process 35 Deg C for ~48 hrs | | | | | Grinding (Mortel and Pestal) | | | | |

OL07-BC3/ x-x cm/ B 375															OL07-BC3/ x-x cm/ B 600			
TOC -Bake ~26 hrs at 375 deg C				BC											Loss on Ignition -Bake ~22 hrs at 600 deg C			
Weight Crucible (g)	Weight Crucible and B375 Before Bake (g)	Weight Crucible and B375 After Bake (g)	TOM %	%CHN - BC	BC- d 13C					%BC					Weight Crucible (g)	Weight Crucible and B600 Before Bake (g)	Weight Crucible and B600 After Bake (g)	Loss on Ignition %
					run 1	run 2	run 3	run 4	Av.	run 1	run 2	run 3	run 4	Av.				
2.3966	2.4502	2.4296	38.43	2.32	-26.374				**-26.374**	1.001953				**1.001953**	2.4202	2.5105	2.4737	40.75
2.373	2.4383	2.4141	37.06	2.41	-26.6887				**-26.6887**	0.802567				**0.802567**	2.3294	2.4657	2.4119	39.47
2.3957	2.4587	2.4343	38.73	1.72	-27.1921				**-27.1921**	0.57564				**0.57564**	2.3809	2.4788	2.4392	40.45
2.3515	2.4115	2.3884	38.50	2.28	-27.2275				**-27.2275**	0.915482				**0.915482**	2.3959	2.5168	2.4675	40.78
2.3607	2.4204	2.3978	37.86	2.84	-27.1784	-25.591	-26.0501997		**-26.2732**	1.135547	1.143625	1.142514		**1.140562**	2.3649	2.4278	2.4022	40.70
2.3882	2.4622	2.4343	37.70	2.59	-26.7211				**-26.7211**	1.091572				**1.091572**	2.3794	2.4809	2.44	40.30
2.3566	2.4262	2.3999	37.79	2.47	-27.2374				**-27.2374**	0.804222				**0.804222**	2.3427	2.49	2.4307	40.26
2.4013	2.4767	2.4481	37.93	2.10	-27.8706				**-27.8706**	0.715717				**0.715717**	2.3426	2.4735	2.4211	40.03
2.342	2.42	2.3905	37.82	1.99	-26.5658				**-26.5658**	0.885753				**0.885753**	2.4149	2.5827	2.5159	39.81
2.3464	2.4032	2.3821	37.15	2.97	-26.8529				**-26.8529**	1.146815				**1.146815**	2.403	2.4855	2.4524	40.12
2.3626	2.4496	2.4164	38.16	2.68	-26.5176				**-26.5176**	1.094613				**1.094613**	2.3833	2.5192	2.4637	40.84
2.3628	2.4493	2.4173	36.99	2.34	-27.139				**-27.139**	1.042732				**1.042732**	2.3399	2.4805	2.4252	39.33
2.3227	2.4066	2.3746	38.14	2.28	-27.3141				**-27.3141**	0.789466				**0.789466**	2.3375	2.4914	2.4292	40.42
2.4471	2.5116	2.4869	38.29	1.94	-26.6818				**-26.6818**	0.780137				**0.780137**	2.38	2.509	2.4571	40.23
2.3649	2.4229	2.4007	38.28	2.34	-25.7192				**-25.7192**	0.766217				**0.766217**	2.296	2.4228	2.3713	40.62
2.3891	2.4575	2.4311	38.60	2.35	-26.4143	-26.77194	-27.5487489	-26.6952	**-26.8576**	0.764178	0.716771	0.703731	0.66278	**0.711865**	2.4594	2.6101	2.5484	40.94
2.3872	2.4729	2.4403	38.04	2.16	-27.0414				**-27.0414**	0.824567				**0.824567**	2.4509	2.5937	2.5363	40.20
2.4213	2.5052	2.4725	38.97	2.17	-26.7103				**-26.7103**	0.727693				**0.727693**	2.3053	2.4827	2.4097	41.15
2.4515	2.5361	2.5034	38.65	2.21	-27.497				**-27.497**	0.790732				**0.790732**	2.3418	2.5055	2.4386	40.87
2.3988	2.4768	2.4462	39.23	2.07	-26.8185				**-26.8185**	1.184876				**1.184876**	2.3957	2.49808	2.4558	41.30
2.3695	2.4375	2.4109	39.12	2.51	-26.4861				**-26.4861**	1.129891				**1.129891**	2.3401	2.4362	2.3962	41.62
2.3621	2.4271	2.4013	39.69	2.20	-26.7821				**-26.7821**	0.765649				**0.765649**	2.3623	2.5146	2.4508	41.89
2.4381	2.5151	2.4849	39.22	2.48	-26.3986				**-26.3986**	0.799314				**0.799314**	2.269	2.4227	2.3586	41.70
2.3787	2.4675	2.432	39.98	2.01	-27.1164				**-27.1164**	0.936027				**0.936027**	2.3297	2.4838	2.4191	41.99
2.3482	2.4236	2.3936	39.79	1.86	-27.2108				**-27.2108**	0.667554				**0.667554**	2.3415	2.499	2.4334	41.65
2.3308	2.4112	2.3791	39.93	2.24	-25.669				**-25.669**	1.115736				**1.115736**	2.3381	2.4543	2.4053	42.17
2.392	2.4722	2.4392	41.15	1.59	-27.8745				**-27.8745**	0.567157				**0.567157**	2.3736	2.5189	2.4568	42.74
2.3995	2.4998	2.4591	40.58	1.97	-28.0476				**-28.0476**	0.663845				**0.663845**	2.3575	2.5521	2.4693	42.55
2.3879	2.481	2.4436	40.17	2.89	-25.9365	-26.49957	-26.0964148	-26.7444	**-26.3192**	1.049241	0.976443	0.961669	0.941084	**0.982109**	2.3744	2.5084	2.4507	43.06
2.3772	2.474	2.4341	41.22	1.35	-26.9768				**-26.9768**	1.184926				**1.184926**	2.3654	2.4502	2.4141	42.57
2.3423	2.4078	2.3802	42.14	2.11	-25.8814				**-25.8814**	0.72642				**0.72642**	2.3329	2.478	2.4138	44.25
2.3647	2.4405	2.4088	41.82	2.07	-26.5028				**-26.5028**	0.597106				**0.597106**	2.3555	2.489	2.4304	43.90
2.3616	2.4377	2.4067	40.74	2.55	-27.0673				**-27.0673**	0.780031				**0.780031**	2.335	2.5533	2.4588	43.29
2.3984	2.3983	2.3984													2.3531	2.56	2.471	43.02
2.4203	2.4979	2.4664	40.59	1.97	-25.4202				**-25.4202**	0.752645				**0.752645**	2.3873	2.548	2.4796	42.56
2.4266	2.5148	2.4788	40.82	1.91	-27.0358				**-27.0358**	0.723361				**0.723361**	2.3689	2.5517	2.4736	42.72
2.3495	2.4295	2.3968	40.88	2.11	-26.1528				**-26.1528**	0.707456				**0.707456**	2.3532	2.53	2.454	42.99
2.3393	2.4029	2.3768	41.04	1.72	-26.0771				**-26.0771**	7.11752					2.3704	2.5617	2.4799	42.76
2.3353	2.4108	2.3796	41.32	1.73	-27.0653	-27.12691	-28.2518084		**-27.4813**	0.632392	0.658361	0.649606		**0.646786**	2.3873	2.5789	2.4964	43.06
2.3774	2.4582	2.4253	40.72	1.84	-26.5392				**-26.5392**	0.695839				**0.695839**	2.4116	2.5634	2.4988	42.56
2.402	2.4785	2.4476	40.39	1.98	-26.5992				**-26.5992**	0.61898				**0.61898**	2.3885	2.5589	2.4867	42.37
2.4043	2.4815	2.4505	40.16	2.09	-25.8401				**-25.8401**	0.719589				**0.719589**	2.3124	2.5001	2.4208	42.25
2.3612	2.4345	2.405	40.25	2.25	-26.8588				**-26.8588**	0.700691				**0.700691**	2.3415	2.5293	2.4495	42.49
2.3719	2.4576	2.4228	40.61	1.74	-27.4065				**-27.4065**	0.626159				**0.626159**	2.3732	2.5274	2.4621	42.35
2.381	2.4407	2.4046	60.47	1.34	-21.5313	-21.05307	-22.8623411		**-21.8156**	2.452794	2.854321	2.677189		**2.661435**	2.4348	2.5419	2.4757	61.81
2.4092	2.5466	2.5341	9.10	3.10	-24.3081				**-24.3081**	0.664971				**0.664971**	2.379	2.607	2.5792	12.19
2.3521	2.6757	2.6397	11.12	2.26	-16.4634	-16.62625	-16.1149365		**-16.4015**	0.250292	0.232619	0.266637		**0.249849**	2.4135	2.9184	2.8508	13.39
2.3932	2.4522	2.395	96.95	2.96	0.976456				**0.976456**	0				**0**	2.4203	2.5345	2.4204	99.91
2.4521	2.4675	2.4639	23.38	74.62	-27.5884	-26.99023	-27.6165966		**-27.3984**	77.85174	84.98183	92.47254		**85.10204**	2.3513	2.3713	2.3517	98.00
2.412	2.5213	2.4832	34.86	5.03	-23.6572	-23.72076	-23.9016892		**-23.7599**	3.081403	2.861564	3.290127		**3.077698**	2.3504	2.4735	2.4244	39.89

OL07-BC3/ x-x cm/ PAH					
	(ng/g_dry)				
	tot. PAHs	me-phen/phen	Fl/(Fl+Pyr)	Retene	% Retene
0.00	797.192	0.892	0.555	637.903	0.800
4.00	806.614	1.011	0.542	693.543	0.860
8.00	448.711	1.115	0.704	346.808	0.773
12.00	345.552	1.087	0.577	236.287	0.684
16.00	1453.332	1.258	0.584	1326.362	0.913
20.00	977.178	1.179	0.544	866.863	0.887
24.00	840.186	1.195	0.577	717.633	0.854
27.00	1289.846	1.119	0.557	1168.177	0.906
34.00	491.345	1.035	0.569	242.104	0.493
37.00	1130.990	1.162	0.539	956.750	0.846
40.00	1228.920	1.146	0.549	1045.492	0.851
43.00	1548.387	1.081	0.538	1335.611	0.863

Appendix D: Burn Records

Example of tree ring scaring used to determine fire records from tree rings (Caprio, Tony)

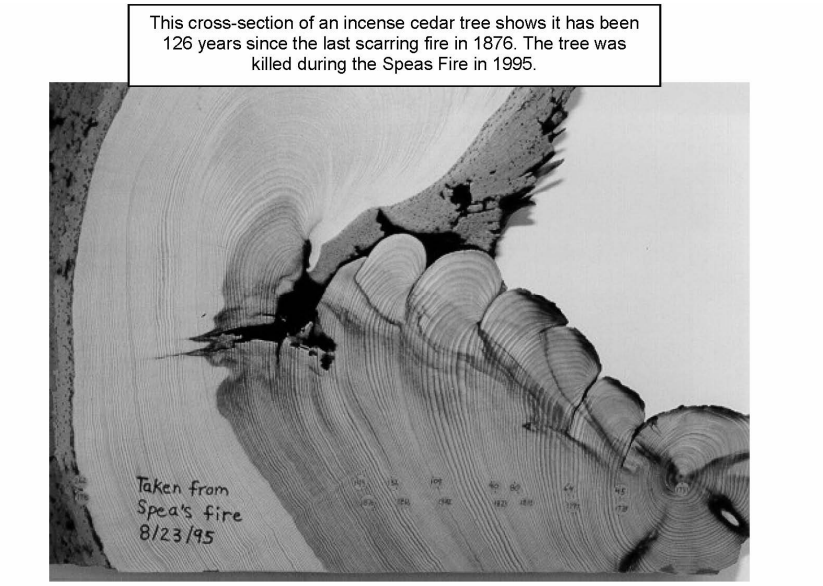

Historic fire record in the Mineral King watershed (Caprio, Anthony C.)

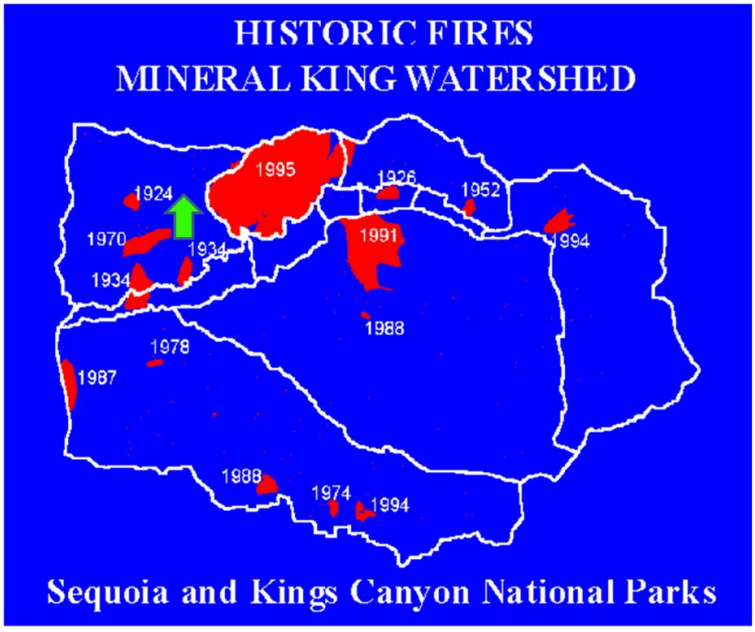

- http://www.nps.gov/archive/seki/fire/frid97.htm

Influence of Fires by Year on Oriole Lake based on Historic Record of Fires											
Year	Influence	Year	Influence	Year	Influence	Year	Influence	Year	Influence	Year	Influence
1919	0	1939	2	1959	5	1979	0	1999	2	2007	0
1918	0	1938	2	1958	5	1978	2	1998	2	2006	0
1917	0	1937	2	1957	5	1977	0	1997	2	2005	0
1916	0	1936	2	1956	5	1976	0	1996	2	2004	0
1915	0	1935	2	1955	5	1975	0	1995	12	2003	0
1914	0	1934	9	1954	5	1974	1	1994	5	2002	5
1913	0	1933	2	1953	5	1973	0	1993	2	2001	5
1912	0	1932	2	1952	6	1972	0	1992	2	2000	5
1911	0	1931	2	1951	5	1971	0	1991	9		
1910	0	1930	2	1950	5	1970	10	1990	2		
1909	0	1929	2	1949	5	1969	0	1989	2		
1908	0	1928	2	1948	5	1968	0	1988	3		
1907	0	1927	2	1947	5	1967	0	1987	7		
1906	0	1926	7	1946	5	1966	0	1986	2		
1905	0	1925	2	1945	5	1965	0	1985	2		
1904	0	1924	12	1944	5	1964	0	1984	2		
1903	0	1923	2	1943	5	1963	0	1983	2		
1902	0	1922	2	1942	5	1962	0	1982	2		
1901	0	1921	2	1941	5	1961	0	1981	2		
1900	0	1920	2	1940	5	1960	0	1980	2		

Appendix E: Other Charts and Graphs.